3D Radiation Pattern Measurement of LTCC Antennas at 60 GHz

D. Titz[1], A. Lamminen[2], M. Kyrö[3], S. M. Azhar[1], F. Ferrero[1], C. Luxey[1], J. Säily[2], G. Jacquemod[1], P. Vainikainen[3]

[1]LEAT-CREMANT-CNRS
University of Nice-Sophia-Antipolis
250, rue Albert Einstein
06560 Valbonne

[2]VTT Technical Research Centre of Finland
P.O. Box 1000, FI-02044 VTT
Finland

[3]Aalto University, SMARAD/Dept. of Radio Science and Engineering
P.O. Box 13000, 00076 Aalto
Finland

***Abstract*-In this paper, we present a fully automatic radiation pattern measurement setup for 60 GHz LTCC antennas. First, a detailed description of the mechanical and the RF parts of the set-up is provided. Then, the 3D radiation pattern measurements of several probe-fed antennas realized on a Low Temperature Co-fired Ceramic (LTCC) substrate are compared with simulations and measurements done at VTT when the antennas are fed by a connector. These experiments demonstrate the possibility to accurately measure the radiation of probe-fed antennas with distinct directions of radiation.**

I. INTRODUCTION

In recent years, the increasing need for higher data rates in consumer applications has raised a lot of interest in developing low-cost radio solutions for millimeter-wave frequencies, especially for the 60 GHz frequency band. Efficient antennas with a wide operational bandwidth are in a key role when fulfilling the link budget requirements at millimeter-wave frequencies. For example, microstrip patch antennas with broadside beams are good candidates for millimeter-wave radios [1]. However, in some specific applications and environments, an end-fire type radiation pattern is more desirable [2]. LTCC has been proven to be a very suitable technology for processing of passive millimeter wave components and antennas on a low loss ceramic substrate. To measure the radiation pattern of such 60 GHz antennas, some solutions exist. But in most of the case, the radiation pattern measurement can only be achieved in limited cut-planes with a manual rotation of the receiving antenna [3-4].

In this paper, we propose to precisely describe and use a fully automatic measurement setup, as in [5], able to measure almost the full 3D radiation pattern of probe-fed antennas in the 60 GHz frequency band. The measurements of those antennas have already been reported when being connector-fed in [1-2]. The antennas are manufactured on LTCC ceramic process and can be integrated with a radio module or flip-chip mounted on a mobile device circuit board. This paper will focus on their radiation pattern measurement, as some of them radiate in the broadside direction and others radiate end-fire beams. The measurement results will be compared with simulations and measurements done at VTT. These experiments demonstrate the possibility to accurately measure the radiation of probe-fed antennas with different directions of radiation.

II. MEASUREMENT SETUP

A schematic view of the setup is presented in Fig. 1. The mechanical part is one of the most innovative pieces of this setup. Two rotating arms made in aluminum are used to scan the sphere around the AUT, the second, being sufficiently rigid to both hold the mixer and the receive horn antenna. To comply with the far field criterion at 60 GHz, the distance between the receive horn and the AUT is chosen to be approximately 20 cm. Therefore, we are able to measure antennas with a largest dimension D being 22 mm. Another important consideration, to be able to accurately measure the radiation below the substrate of the AUT, is to get rid of the metallic chuck usually used in probe-based measurements for microelectronics [4], because such a large piece of reflective material affects strongly the radiation. Our system uses specifically fabricated FR4 or foam AUT holders which are screwed to a special rigid polyurethane carrier. This carrier helps greatly in maintaining the metallic positioner as far as possible from the volumic area to be scanned (Fig. 2).

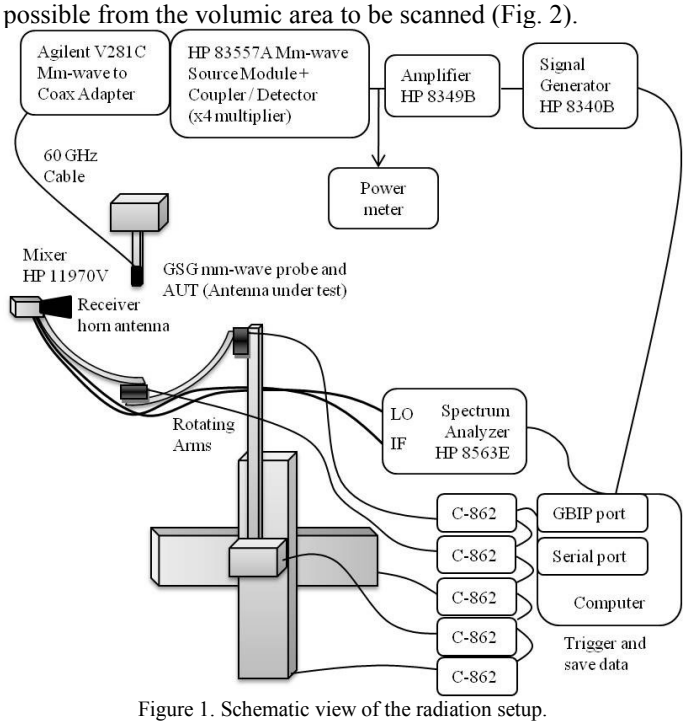

Figure 1. Schematic view of the radiation setup.

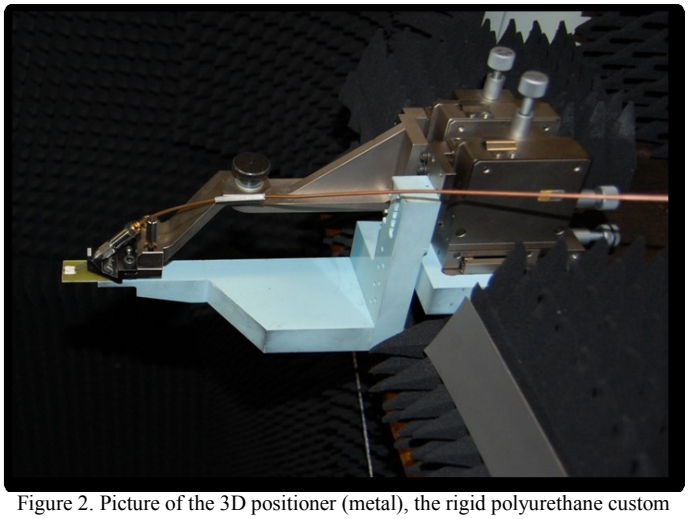

Figure 2. Picture of the 3D positioner (metal), the rigid polyurethane custom made carrier (blue) and a special FR4 holder for an LTCC antenna.

This setup fits in less than $1m^3$ and the synthesizer, spectrum analyzer, the rotation and the translation of the arms trough servo-motors are all controlled by a computer (GPIB and serial port), using a custom-made Labview code. The total 3D measurement of one antenna is completed in 2 hours. The setup has an overall uncertainty of ± 1 dB for the computed realized gain of any antenna.

III. LTCC End-Fire Antenna Element

A. Design

The first 60 GHz antenna presented in this work is a planar dipole embedded inside an LTCC substrate and is fed by a microstrip line on the top. The operation of the antenna is based on radiation of a TE_0 surface wave, launched by the dipole, from a finite substrate having a high dielectric constant of 5.9 such as LTCC. A slot at the center of the microstrip ground plane acts as a balun and provides the differential feed for the dipole element [6]. The reactive part of the input impedance is controlled with an open stub similar to the one used, for example, in an aperture-coupled patch antenna. A reflector, i.e., a wide ground plane can be used on the lower part (-y-direction) of the antenna to obtain radiation into the upper hemisphere (+y-direction). For more omni-directional operation, the reflector can be excluded.

The end-fire antenna was optimized to have wideband impedance characteristics and a broad radiation pattern using the commercial EM simulator Ansoft HFSS. The antenna consists of three Ferro A6-M LTCC tape layers having $\varepsilon_r = 5.9$, $tan\delta = 0.0015$, and the tape thickness $h_1 = 90\ \mu m$. Used gold paste has a conductivity of $\sigma_{Aup} = 7.0.10^6\ S/m$. The antenna simulation model is shown in Fig. 3.

B. Reflection Coefficient Measurement

The reflection coefficient of the antenna element was measured on a probe station using a GSG probe with 150 µm pitch. The measurement results are shown in Fig. 4 together with the simulated ones.

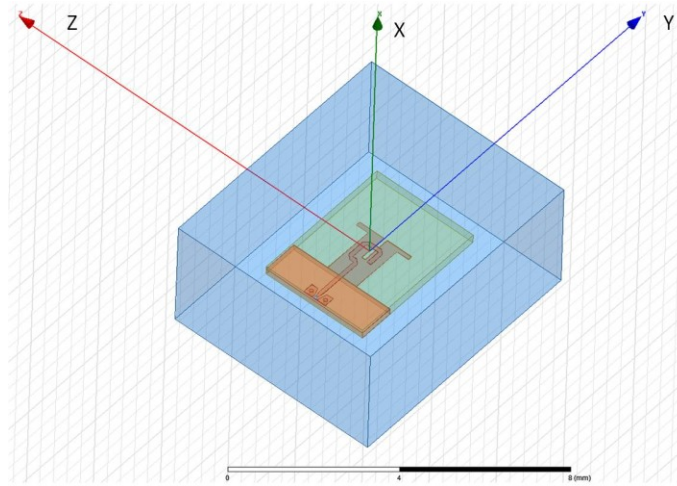

Figure 3. End-fire antenna simulation model in HFSS with corresponding coordinate system.

Simulations were carried out with microstrip-mode excitation (”wave”) using a wave port in the HFSS. Another simulation (”lump”) was done in which the GSG probe pads were included and a lumped port was used as the excitation. It is seen that the probe transition shifts the center frequency downwards but the $|S_{11}|$ remains good in shape. The LRRM calibration standards were used in the measurements and the effect of the probe pads is seen in the results. Three samples were measured and the results are very similar with each other. The double resonance behavior is observed. The measured $|S_{11}|$ is below 10 dB between 53– 59 GHz and 65–68 GHz and rises to a maximum value of 6.8 dB at 62 GHz.

The difference between the simulated and the measured results is partly due to the manufacturing tolerances. Also, unfortunately, the probe pads of the diced antenna sample were short-circuited and the measurements had to be done from the undiced panels in which the nearby test structures may have some effect on the $|S_{11}|$ of the antenna under test.

C. Radiation Pattern Measurement

Radiation patterns were measurement in VTT’s anechoic chamber and with the LEAT setup presented in Sec. II. A special foam holder was fabricated for the antenna (Fig. 5). Radiation pattern measurement made in VTT of this antenna had already been published in [2]. Hence, we will focus this part on the measurement results obtained with the setup presented in Sec. II.

The simulated and measured radiation patterns of the antenna element in the E- and H-plane are shown in Fig. 6-8. The H-plane and E-plane respectively correspond to the XY and YZ planes in Fig. 3. The patterns compare very well with the simulations. The cross-polarization level is below -10 dBi in the H- and E-planes at 60 GHz. As can be seen in Figs. 6-8, only a part of the E and H planes can be measured. This is due to the way the antenna is fed. The use of a microelectronic probe forbids us to move the antenna during the measurement. Hence, we cannot measure behind the probe where the micro-positioner lies (Fig. 2). The magnitude difference in the E plane around Theta=330° is due to the probe itself which is

blocking the signal coming from the antenna and going to the receive horn antenna (Fig. 8).

As the match between simulation and measurement results is very good, we want to compare two sets of measurement data. The first one is provided by VTT and the antenna is then fed by a connector. A thin absorber sheet has to be inserted between then antenna and the connector to suppress any reflections from the metal connector. From [2], we can see that the coincidence between simulation and measurement is also very good. Fig. 9 shows both measurement data. From these figures, we can hardly say if one setup is better than the other. However, we can raise some points. In the H-plane around Phi=0° and 180°, the values of the gain from the LEAT measurement are a bit higher than the ones obtained with the VTT measurement. But, looking at Fig. 6, they match the simulation data. The lower gain in the VTT measurement can be explained by the way the antenna is fed during the measurement. The absorber sheet may be interacting with the measurement by loading the near-field of the AUT. However, with the VTT set-up, the measurement of the whole H and E planes is possible.

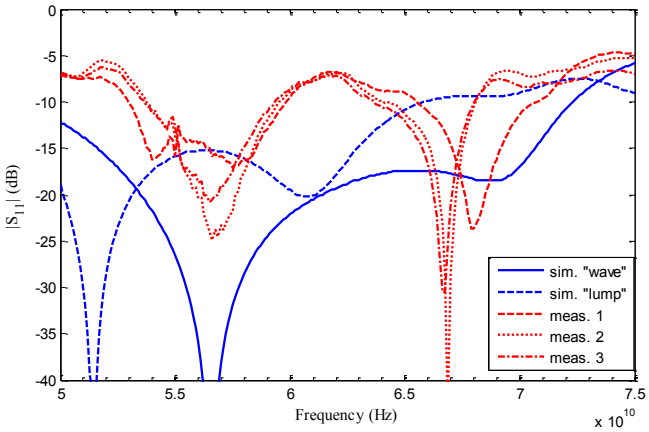

Figure 4. Simulated and measured (probe station) reflection coefficients of the end-fire antenna.

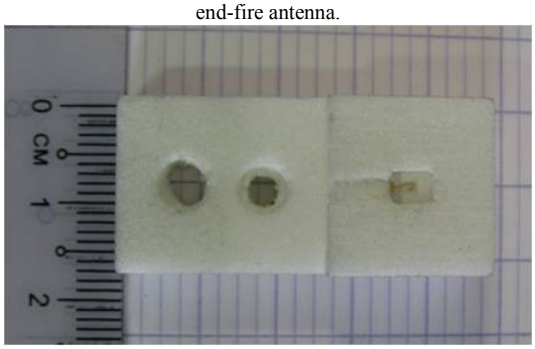

Figure 5. End-fire antenna and foam holder.

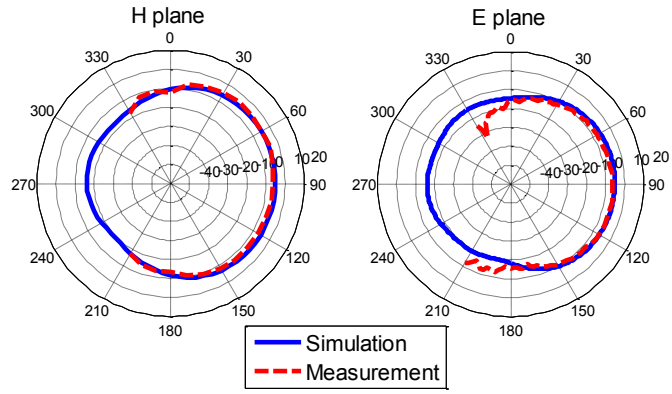

Figure 6. Simulated (blue solid line) and measured in LEAT (red dashed line) end-fire antenna co-polarization gain patterns at 60 GHz. The scale is from -50 dBi to 20 dBi with 10 dBi steps.

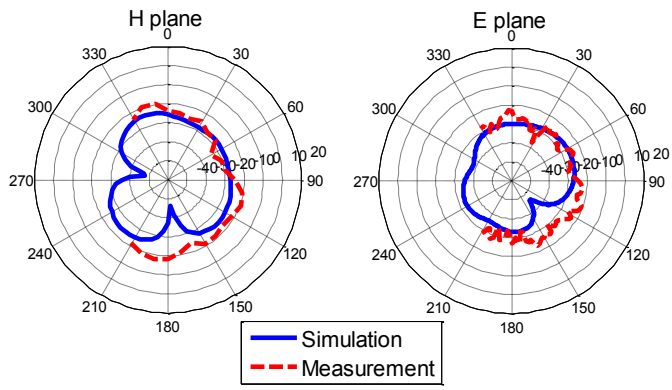

Figure 7. Simulated (blue solid line) and measured in LEAT (red dashed line) end-fire antenna cross-polarization gain patterns at 60 GHz. The scale is from -50 dBi to 20 dBi with 10 dBi steps.

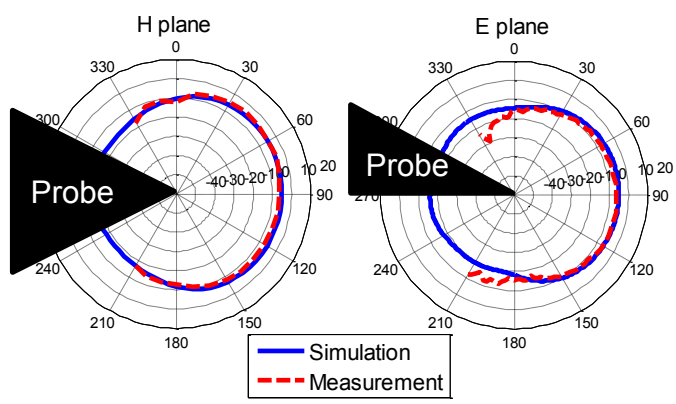

Figure 8. Simulated (blue solid line) and measured in LEAT (red dashed line) end-fire antenna total gain patterns at 60 GHz. The scale is from -50 dBi to 20 dBi with 10 dBi steps.

Finally, the LEAT setup is able to provide almost full 3D radiation pattern. Fig. 10 shows a comparison between simulation and measurement results of the end-fire antenna. The two data patterns are really close to each other. We obtained a simulated maximum total gain of 4.96 dBi in the direction Phi=125° and Theta=88° and a measured maximum total gain of 6.27 dBi in the direction Phi=140° and Theta=74°.

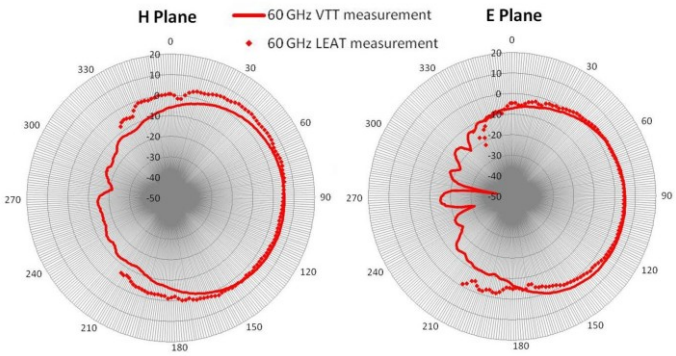

Figure 9. Measured in VTT (red solid line) and measured in LEAT (red dashed line) end-fire antenna co-polarization gain patterns at 60 GHz. The scale is from -50 dBi to 20 dBi with 10 dBi steps.

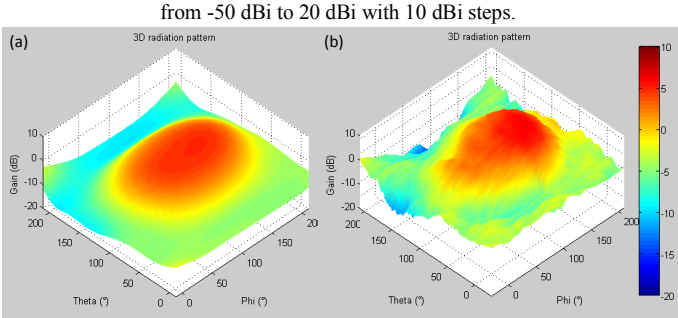

Figure 10. Simulated (a) and measured in LEAT (b) end-fire antenna total 3D gain patterns at 60 GHz. The scale is from -20 dBi to 10 dBi with 5 dBi steps.

IV. LTCC End-Fire Antenna Array

A. Design

The endfire antenna geometry enables its use in an antenna array. A small 1x4 linear array was designed in order to obtain a fan-shaped beam, i.e., a narrow radiation pattern in the horizontal plane and a wide beam in the azimuth plane, and therefore a higher total gain. A microstrip-line feed network was designed and Wilkinson power dividers were used to distribute power equally between elements (Fig. 11).

B. Reflection Coefficient Measurement

The simulated and measured reflection coefficients of the array are displayed in Fig. 12. The simulated and measured results of three samples agree very well with each other.

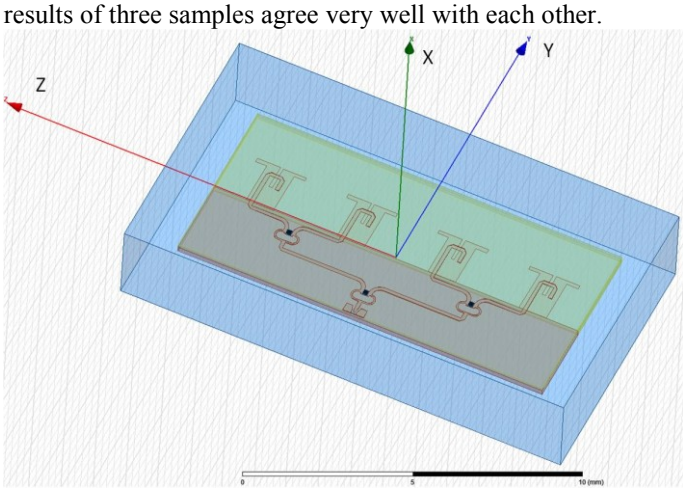

Figure 11. End-fire antenna array simulation model in HFSS with corresponding coordinate system.

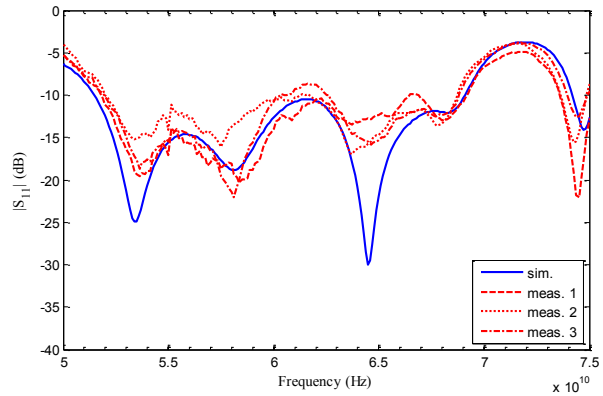

Figure 12. Simulated and measured (probe station) reflection coefficients of the end-fire antenna array.

C. Radiation Pattern Measurement

Radiation patterns were measured in VTT's anechoic chamber and with the LEAT setup. A special foam holder was fabricated for the antenna (Fig. 13). Radiation pattern measurement made in VTT of this antenna had already been published in [2]. Hence, we will focus on the measurement results obtained with the LEAT setup.

The simulated and measured radiation patterns of the antenna element in the E- and H-plane are shown in Fig. 14-16. The H-plane and E-plane respectively correspond to the XY and YZ planes in Fig. 11. The patterns compare very well with the simulations.

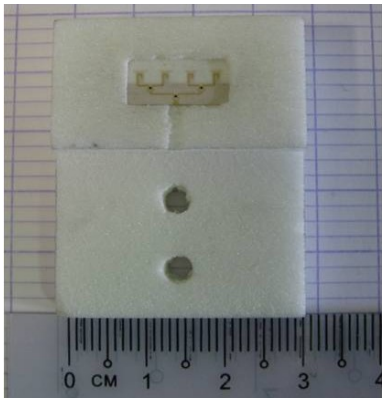

Figure 13. End-fire antenna array and foam holder.

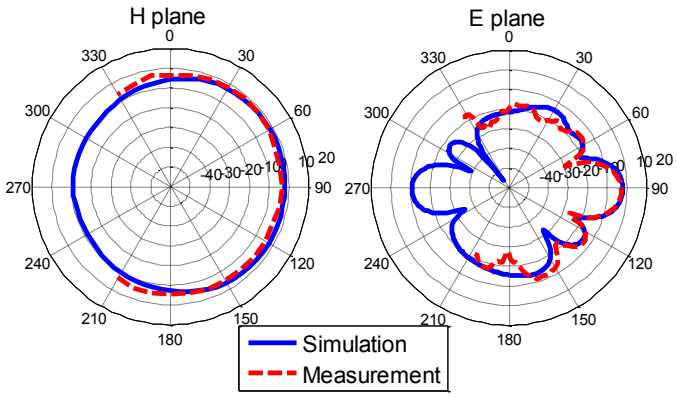

Figure 14. Simulated (blue solid line) and measured in LEAT (red dashed line) end-fire antenna array co-polarization gain patterns at 60 GHz. The scale is from -50 dBi to 20 dBi with 10 dBi steps.

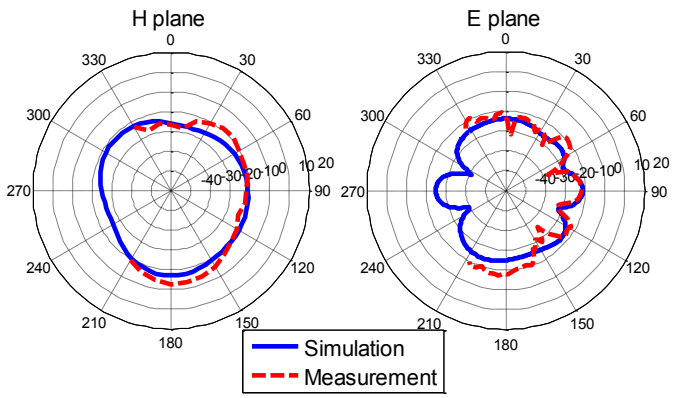

Figure 15. Simulated (blue solid line) and measured in LEAT (red dashed line) end-fire antenna array cross-polarization gain patterns at 60 GHz. The scale is from -50 dBi to 20 dBi with 10 dBi steps.

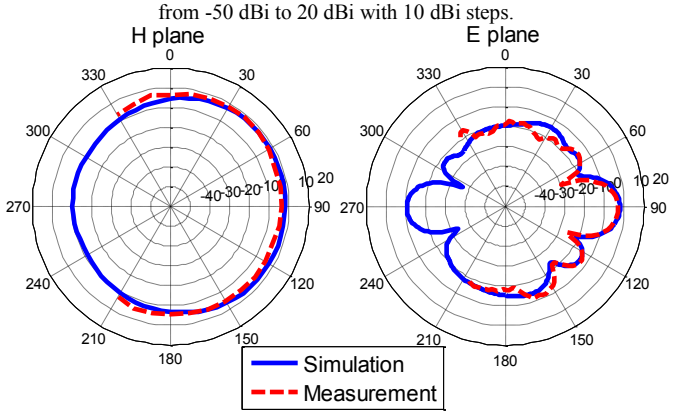

Figure 16. Simulated (blue solid line) and measured in LEAT (red dashed line) end-fire antenna array total gain patterns at 60 GHz. The scale is from -50 dBi to 20 dBi with 10 dBi steps.

As the match between simulation and measurement results is very good, we want to compare the two sets of measurement data. The first one is provided by VTT. The antenna is then fed by a connector. From [2], we can see that the comparison between simulation and measurement is also very good. Fig. 17 shows both measurement data.

Fig. 18 shows a comparison between simulation and measurement of the end-fire antenna. The two patterns are really close to each other. The side lobes are more pronounced in the measurement. We obtained a simulated maximum total gain of 8.27 dBi in the direction (Phi=130° and Theta=91°) and a measured maximum total gain of 8.76 dBi in the direction (Phi=140° and Theta=92°).

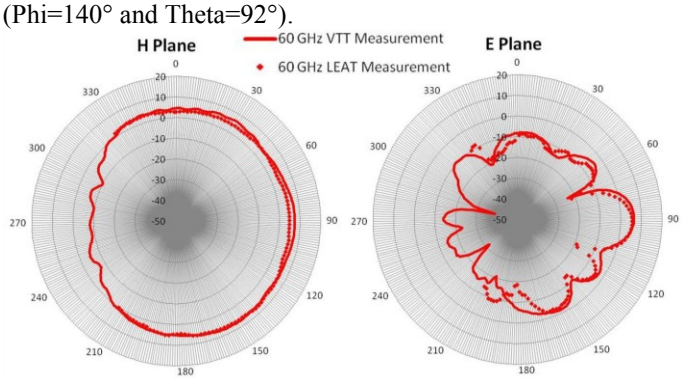

Figure 17. Measured in VTT (red solid line) and measured in LEAT (red dashed line) end-fire antenna array co-polarization gain patterns at 60 GHz. The scale is from -50 dBi to 20 dBi with 10 dBi steps.

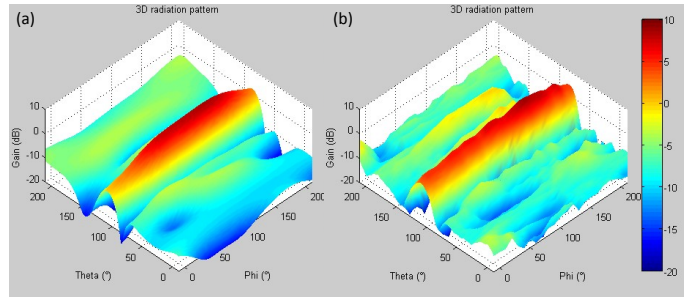

Figure 18. Simulated (a) and measured in LEAT (b) end-fire antenna array total 3D gain patterns at 60 GHz. The scale is from -20 dBi to 10 dBi with 5 dBi steps.

V. LTCC Patch Array

A. Design

The LTCC patch antenna array has already been published in [1]. But, no measurement of this antenna had been performed. The antenna consists of a 2x2 planar array of aperture-coupled microstrip line-fed patch antennas (ACMPAs). The arrays are excited through the microstrip-line feed networks using Wilkinson power dividers. The antenna simulation model is shown in Fig. 19.

B. Reflection Coefficient Measurement

The simulated and measured reflection coefficients of ACMPA array are displayed in Fig. 20.

C. Radiation Pattern Measurement

No measurement of this antenna was performed in VTT. So, in this part, we will only compare the measurements results obtained in Nice to the simulation data. The simulated and measured radiation patterns of the antenna element in the E- and H-plane are shown in Fig. 21. The H-plane and E-plane respectively correspond to the XY and XZ planes in Fig. 19. The patterns compare very well with the simulations.

As can be seen in Fig. 21, only a part of the H plane can be measured because of the probe feeding technique, but the whole E plane can be measured. Side lobes seem higher in the measurement than in simulation.

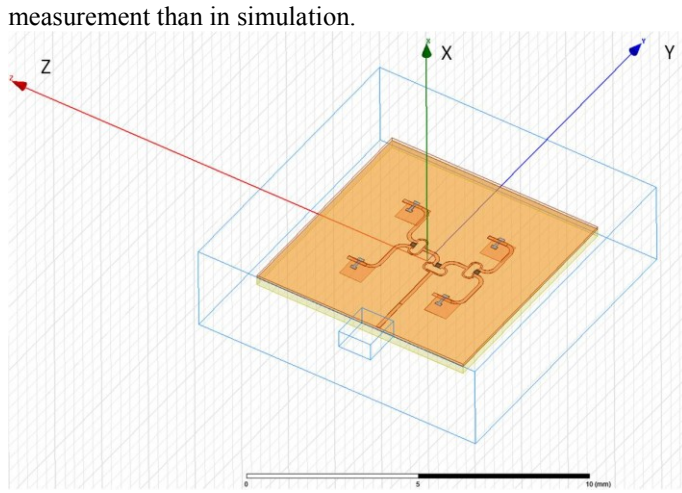

Figure 19. ACMPA array simulation model in HFSS with the corresponding coordinate system.

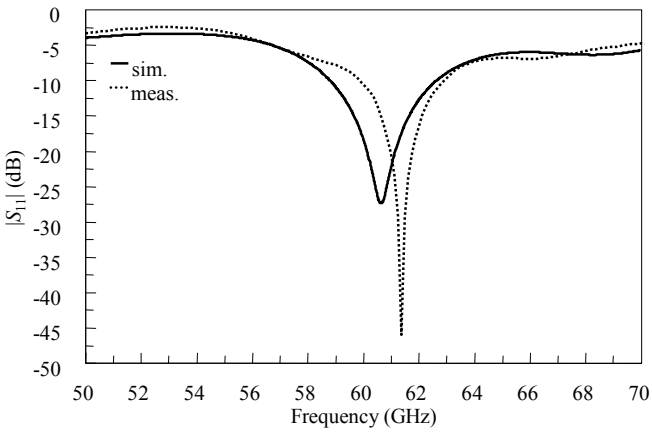

Figure 20. Simulated and measured reflection coefficients of the ACMPA array.

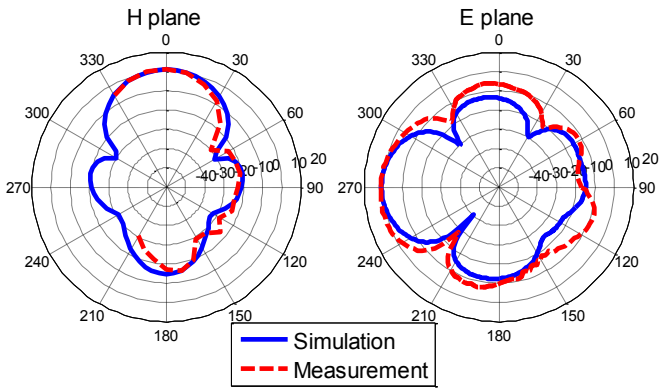

Figure 21. Simulated (blue solid line) and measured in LEAT (red dashed line) ACMPA array co-polarization gain patterns at 60 GHz. The scale is from -50 dBi to 20 dBi with 10 dBi steps.

Fig. 22 shows a comparison between simulation and measurement of the 3D gain pattern of the ACMPA array. The two patterns are really close to each other. The side lobes are more pronounced in the measurement and the main lobe seems broader. We obtained a simulated maximum total gain of 10.9 dBi in the direction (Phi=190° and Theta=90°) and a measured maximum total gain of 11.8 dBi in the direction (Phi=180° and Theta=96°).

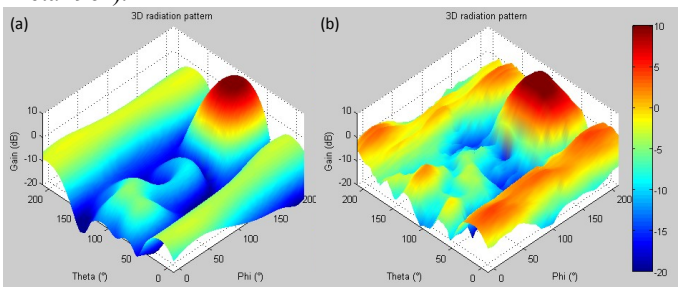

Figure 22. Simulated (a) and measured in LEAT (b) ACMPA array total 3D gain patterns at 60 GHz. The scale is from -20 dBi to 10 dBi with 5 dBi steps.

VI. Conclusion

In this paper, we have presented a radiation pattern measurement setup dedicated to 60 GHz probe-fed integrated antennas. It uses microelectronic probes to feed the antenna under test. Using this setup, several LTCC antennas were measured. The first antennas [2] to be measured are end-fire antennas. They had already been measured in VTT facilities using a different feeding technique (connector). Both measurements gave results close to simulation data. We particularly show the accuracy of the setup in the broadside direction. The last antenna uses a patch-type structure [1]. As this antenna is fed from the top side of the LTCC substrate but radiates from the back side, it demonstrated the accuracy of the setup for measurement below the antenna under test. We specifically targeted two antenna structures with different directions of main radiation. But, more than the ability of the setup to measure the almost full 3D radiation pattern this work showed that the accuracy of the setup is good in any directions.

Acknowledgment

The authors would like to thank the CIMPACA design platform and the CREMANT for their financial and technical support.

References

[1] A. E. I. Lamminen, J. Säily, and A. R. Vimpari, “60-GHz patch antennas and arrays on LTCC with embedded-cavity substrates”, *IEEE Trans. Antennas Propag.*, vol. 56, no. 9, pp. 2865-2874, Sept. 2008.

[2] A. E. I. Lamminen, and J. Säily, “Wideband millimeter wave end-fire antenna and array for wireless short-range applications”, *European Conference on Antennas and Propagation 2010*, Barcelona, Spain, April 2010.

[3] J.A.G. Akkermans, R. van Dijk, and M.H.A.J. Herben, “Millimeter-wave antenna measurement”, *European Microwave Conference 2007*, pp. 83-86, Munich, Germany, October 2007.

[4] R. Pilard, S. Montusclat, D. Gloria, F. Le Pennec, and C. Person, “Dedicated measurement setup for millimetre-wave silicon integrated antennas: BiCMOS and CMOS high resistivity SOI process characterization”, *European Conference on Antennas and Propagation 2009*, pp. 2447-2451, Berlin, Germany, March 2009.

[5] S. Ranvier, M. Kyrö, C. Luxey, C. Icheln, R. Staraj, and P. Vainikainen, “Compact 3-D on-wafer radiation pattern measurement system for 60 GHz antennas”, *Microwave and Optical Technology Letters*, vol. 51, pp. 319-324, February 2009.

[6] K. M. K. H. Leong, Y. Qian, and T. Itoh, “Compact surface-wave assisted printed endfire antenna with multiple system compatibility,” in *IEEE Antennas and Propagation Society International Symposium Digest*, Boston, MA, July 2001, pp. 448–451.